RESEARCH ARTICLE

Patient dose reduction for a localizer radiograph with an additional tin filter in chest–abdomen–pelvis, spine, and head computed tomography examinations

Masaki Takemitsu[1] · Kazuki Takegami[1,2] · Shohei Kudomi[1] · Kaito Kawanami[1]

Abstract

This study aimed to evaluate the dose reduction potential of adding a tin filter to localizer radiographs (LR) on computed tomography (CT) examinations in both phantom and clinical studies. LRs were performed using combinations of 120 kVp and 20 mA (120/20), 100 kVp with a tin filter, and 50 mA or 20 mA (Sn100/50, Sn100/20). For the phantom experiment, entrance surface doses (ESD) of the LRs were evaluated for each protocol using an anthropomorphic phantom. This retrospective clinical study included 700 patients (300 for chest–pelvis, 200 for spine, and 200 for head CTs). The volume CT dose indices ($CTDI_{vol}$s) of the main CT scans were recorded and placed into one of three groups based on body mass index (BMI): underweight, normal-weight, and overweight, to evaluate the effect of LR acquisition conditions on the performance of the automatic tube current modulation technique of subsequent CT scans. The ESDs of all LRs with the Sn100/50 protocol were 0.03 mGy, a decrease of more than 80% compared to those of the 120/20 protocol. Moreover, the Sn100/20 protocol reduced ESD to 0.02 mGy. In chest–pelvis CT, there were no significant differences in the $CTDI_{vol}$ between with and without a tin filter for each BMI group. However, the lateral LRs with the tin filter on the spine CT slightly reduced the $CTDI_{vol}$ in normal-weight and overweight patients. Although there is room to optimize the acquisition conditions for larger patients, an additional tin filter for LR is a useful means to efficiently reduce ESDs.

Keywords Computed tomography · Localizer radiograph · Tin filtration · Dose reduction

1 Introduction

Improvements in computed tomography (CT) scanning techniques, such as using a low tube voltage [1] and an additional filter [2–4], allow us to effectively reduce radiation doses in patients. Consequently, particularly for low-dose CT scans, there are cases in which the doses of the main CT scans are close to those of localizer radiograph (LR) acquisition. Therefore, more attention has been paid to furthering radiation dose reduction in LR acquisitions [5–8].

LRs were acquired to determine the scan range of a subsequent CT scan and optimize the performance of the automatic tube current modulation (ATCM) technique. If these settings are properly achieved, the radiation dose of LR acquisition should be reduced as low as possible because LRs are generally not used for clinical diagnosis. Some reports have indicated that the radiation dose of LRs can be reduced using optimal scan parameters (e.g., low tube voltage and low tube current) [9, 10]. Bohrer et al. [11] showed that optimizing LR acquisition with a low tube voltage and current reduced the patient dose by more than 90%. Moreover, Saltybaeva et al. [12] reported that tin spectral shaping filtration can be applied to LRs to further reduce the radiation dose without negatively impacting the performance of ATCM, although patient size should be considered. However, most of these studies used anthropomorphic phantoms

✉ Masaki Takemitsu
  take-555@yamaguchi-u.ac.jp

  Kazuki Takegami
  kazuki-t@yamaguchi-u.ac.jp

  Shohei Kudomi
  kudomi@yamaguchi-u.ac.jp

  Kaito Kawanami
  kai-0514@yamaguchi-u.ac.jp

1 Department of Radiological Technology, Yamaguchi University Hospital, Yamaguchi 755-8505, Japan

2 Graduate School of Medical Sciences, Kanazawa University, Ishikawa 920-0942, Japan

and did not address the application of low-dose LR acquisition to patients in a clinical setting. This study aimed to evaluate the feasibility of dose reduction during LR using tin filter technology in chest-to-pelvis (chest–pelvis), spine, and head CT examinations. We assessed the reduction in radiation dose in acquiring LRs and the effect of scan parameters of LRs on the ATCM in the main CT scans using a phantom experiment and a clinical study.

2 Materials and methods

A third-generation dual-source CT (SOMATOM Force, Siemens Healthineers, Forchheim, Germany) was used for both the phantom and clinical studies. In this scanner, a tin filter that omits lower energies to reduce radiation doses can be used not only for the main CT scans, but also for the acquisition of LRs [13, 14]. The following sections describe two verifications: (1) the radiation doses for LR acquisition using a phantom in the phantom study, and (2) the effect on the performance of the ATCM of the subsequent CT scan in the clinical study.

2.1 Phantom experiment

We evaluated the typical radiation doses of the LRs during chest–pelvis, spine, and head CT examinations using an anthropomorphic phantom (THRA-1, Kyoto Kagaku Co., Ltd., Kyoto, Japan). The entrance surface dose (ESD) was measured using a sufficiently annealed optically stimulated luminescence (OSL) dosimeter (nanoDot™, Landauer Inc., Illinois, USA) to evaluate the maximum radiation dose. As shown in Fig. 1a, b, c, dosimeters were placed on the anterior

surface of the abdomen at the level of the umbilicus, the lateral surface of the abdomen at the level of the umbilicus, and the lateral surface of the temporal bone in the chest–pelvis, spine, and head CT examinations, respectively. LRs were acquired using the following tube voltages and tube currents: 120 kVp and 20 mA (settings commonly used in clinical situations) as a reference protocol (120/20) and 100 kVp with a tin filter (Sn100 kVp) and 50 mA as a study protocol (Sn100/50) (Table 1). In addition, LR for the chest–pelvis CT examination was also performed with Sn100 kVp and 20 mA as the lowest dose protocol (Sn100/20). The scanning regions of the LRs were determined to include the apex of the lungs to the pubic joint for the chest–pelvis and spine CT, and the whole brain for the head CT. Dose measurements were performed three times for each experiment.

Table 1 Scan conditions of LR acquisition performed on the chest–pelvis, spine, and head CT examinations

Name of protocols		Scan conditions of LRs		
Region	Protocol	Tube voltage [kVp]	Tube current [mA]	Direction
Chest–pelvis CT	120/20	120	20	AP*
	Sn100/50	Sn100	50	
	Sn100/20	Sn100	20	
Spine CT	120/20	120	20	Lat
	Sn100/50	Sn100	50	
Head CT	120/20	120	20	Lat
	Sn100/50	Sn100	50	

AP indicated anteroposterior; Lat, lateral

*In the clinical study, LRs for CAP-CT were scanned at posteroanterior direction

Fig. 1 Experimental setup for measuring entrance surface dose. OSL dosimeters were placed on the surface of an anthropomorphic phantom

a. Chest-Pelvis CT   b. Spine CT   c. Head CT
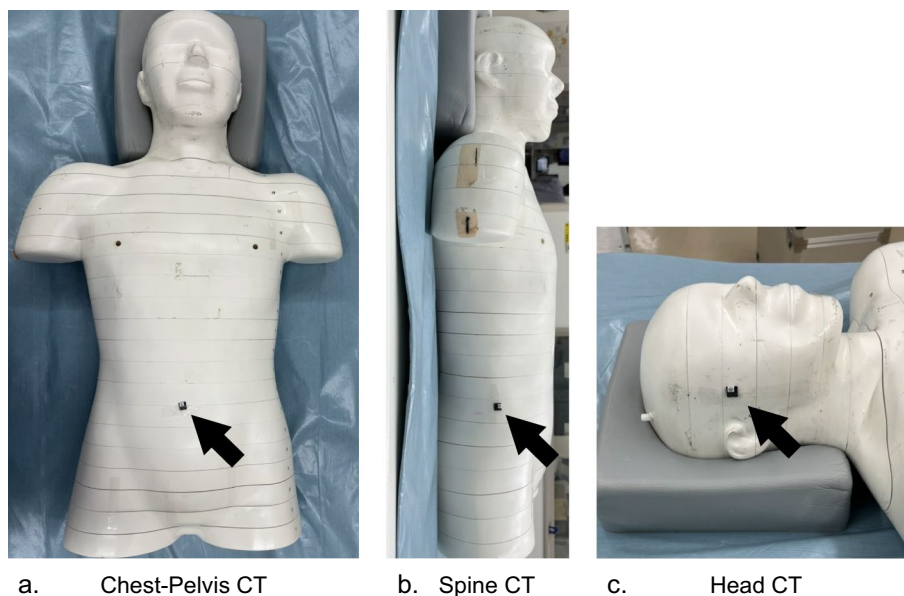
This section describes the analysis procedure used to derive the ESD using the OSL dosimeter. Using a reading device (microSTAR®ii, Landauer Inc., Illinois, USA), we obtained the OSL response as counts. The ESD was calculated as $ESD = \frac{Counts}{CF}$, where CF was a dose calibration factor that was determined based on a previously reported procedure [15, 16]. In this study, the calibration factors of 120 kVp and Sn100 kVp under free-air conditions were determined as CF_{120kVp}=944 mGy^{-1} and $CF_{Sn100kVp}$=767 mGy^{-1}, respectively. The margin of error of the ESD when using the factors in the CT scans was evaluated by considering the uncertainty of the calibration procedure (5%) [16], statistical error (square root of the counts) of the counts, and the standard deviation of the three measurements.

2.2 Clinical study

A clinical study was performed to evaluate the effect of scan conditions on the performance of the ATCM for subsequent CT scans. The Institutional Review Board of our hospital approved this research. LR acquisition with the tin filter was available in our CT scanner after a software update in April 2019, and subsequently, the acquisition was applied to all CT examinations. We retrospectively evaluated the consecutive data of 700 patients who underwent CT examinations with and without a tin filter between November 2016 and September 2021 (300 for chest–pelvis CT, 200 for spine CT, and 200 for head CT). The scan conditions for LRs were the same as those of the phantom experiment, except for the direction of irradiation in the chest–pelvis CT (Table 1); that is, the posteroanterior direction was used instead of the anteroposterior direction. Using the LR, the scan region of the subsequent CT scan was determined, and the scan was performed using an ATCM system (CARE Dose 4D, Siemens Healthineers, Germany). The scan parameters and ATCM settings for the main CT scans for each CT examination are shown in Table 2. For analysis of results, the average volume CT dose indices (CTDI$_{vol}$s) of the main CT scans were recorded and categorized into the following three groups using body mass index (BMI): underweight (< 20 kg/m^2), normal-weight ($20 - 24.9$ kg/m^2), and overweight (≥ 25 kg/

Table 3 Experimental results of entrance surface dose measurements in LR acquisitions for each protocol

Protocols of LRs			Entrance surface dose [mGy]
Region	Protocol	Direction	
Chest–pelvis CT	120/20	AP	0.17 ± 0.01
	Sn100/50		0.03 ± 0.01
	Sn100/20		0.02 ± 0.01
Spine CT	120/20	Lat	0.18 ± 0.02
	Sn100/50		0.03 ± 0.01
Head CT	120/20	Lat	0.16 ± 0.01
	Sn100/50		0.03 ± 0.01

AP indicated anteroposterior; Lat, lateral

m^2). BMI was calculated by dividing body weight (kg) by height squared (m^2). The CTDI$_{vol}$s for each BMI group were compared for each LR scan condition.

2.3 Statistical analysis

Categorical variables are reported as frequencies and percentages. Continuous variables are reported as averages and standard deviations for those with a normal distribution and as medians and interquartile ranges (IQR) for those with a non-normal distribution. Patient characteristics were compared using one-way analysis of variance (ANOVA) and Welch's t-test for age, height, weight, and BMI. The Mann–Whitney U test was used to test for significant differences in the CTDI$_{vol}$ results. Statistical significance was set at $p < 0.05$. All statistical analyses were performed using the JMP 14.0.0 software (SAS Institute, Cary, NC, USA).

3 Results

3.1 Phantom study

Table 3 shows the experimental results of the ESD measurements when the LR was acquired. During chest–pelvis CT, the ESD was 0.17 mGy in the reference protocol (120/20).

Table 2 Scan conditions of the main CT scans performed on chest–pelvis, spine, and head CT examinations

Name of protocols	Scan conditions of main scans				
Region	Tube voltage [kVp]	Quality reference mAs [mAs]	Pitch factor	Rotation time [s]	Beam collimation [mm]
Chest–pelvis CT	Care kV*	180	0.6	0.5	192×0.6
Spine CT	120	250	0.8	1.0	192×0.6
Head CT	120	420	0.55	1.0	192×0.6

The tube voltage was automatically selected from 90 to 120 kVp by automatic tube voltage selection (Care kV, Siemens Healthineers, Germany)

For the Sn100/50 and Sn100/20 protocols using tin filter technology, the ESDs were 0.03 and 0.02 mGy, respectively; that is, the corresponding reduction rates were approximately -80% and -90%. The results of spine and head CT showed a similar trend to those of the chest–pelvis CT. The ESDs of the 120/20 and Sn100/50 protocols during spine CT were 0.18 and 0.03 mGy, and during head CT were 0.16 and 0.03 mGy, respectively. The dose reduction rates for spine and head CT scans with the tin filter were approximately -80%.

3.2 Clinical study

There were no significant differences in patient characteristics, including age, height, weight, and BMI, between the scanning conditions (Table 4). Figure 2 shows the box plots of $CTDI_{vol}$ recorded in the chest–pelvis CT examinations, which were scanned based on LR acquisitions in 120/20, Sn100/50, and Sn100/20 protocols. Figure 2a, b, c represents the results of the three BMI groups divided

into underweight, normal-weight, and overweight groups, respectively. The mean $CTDI_{vol}$s for each protocol increased as the BMI increased. In all BMI groups, there were no significant differences in $CTDI_{vol}$ between the 120/20 and Sn100/50 protocols (underweight, $p=0.95$; normal-weight, $p=0.49$; overweight, $p=0.99$). Moreover, the results of the Sn100/20 protocol were not significantly different from those of the 120/20 protocol (underweight, $p=0.40$; normal-weight, $p=0.52$; overweight, $p=0.31$). The typical LRs of the three BMI groups and protocols are shown in Fig. 3.

In the spine CT examinations for the underweight group, no significant differences in $CTDI_{vol}$ were found between the 120/20 and Sn100/50 protocols ($p=0.22$) (Fig. 4a). However, for the normal-weight and overweight groups, the $CTDI_{vol}$s in the Sn100/50 protocol were statistically lower than those in the 120/20 protocol (normal-weight: 12.06 ± 1.14 mGy vs. 14.10 ± 1.42 mGy, $p<0.01$; overweight: 14.58 ± 1.66 mGy vs. 17.86 ± 3.57 mGy, $p<0.01$) (Fig. 4b, c). Figure 5 shows typical images of spine CT. As indicated by the black arrows, the anatomical structure of

Table 4 Patient characteristics of CT examinations for each protocol

Characteristic	Chest–pelvis CT				Spine CT			Head CT		
	120/20	Sn100/50	Sn100/20	P value	120/20	Sn100/50	P value	120/20	Sn100/50	P value
No. of patients	100	100	100		100	100		100	100	
Age [y]	70.5 ± 13.3	71.4 ± 11.9	69.2 ± 12.5	0.47	67.2 ± 14.0	67.5 ± 14.4	0.90	67.7 ± 16.4	67.8 ± 16.7	0.97
Male/female	72/28	63/37	62/38		51/49	52/48		63/37	55/45	
Height [cm]	161.5 ± 9.1	160.5 ± 8.3	160.6 ± 8.5	0.67	159.1 ± 10.0	158.9 ± 9.5	0.89	160.7 ± 9.7	159.7 ± 10.3	0.49
Weight [kg]	60.4 ± 13.2	59.8 ± 12.1	59.4 ± 11.2	0.84	63.8 ± 15.6	60.4 ± 13.4	0.11	60.0 ± 14.6	58.3 ± 13.1	0.37
BMI [kg/m²]	23.0 ± 3.7	23.2 ± 4.0	59.4 ± 11.2	0.91	25.1 ± 5.4	23.8 ± 4.1	0.06	23.1 ± 4.8	22.8 ± 4.2	0.57

Unless otherwise specified, data are shown in the form of mean value ± standard deviation

Fig. 2 Results of the clinical study during chest–pelvis CT examinations. **a**, **b**, and **c** The box and whisker plots of $CTDI_{vol}$s for patients who were underweight, normal-weight, and overweight, respectively, in each protocol. There were no significant differences in the $CTDI_{vol}$s with and without the tin filter technology

a. Underweight (BMI<20)
b. Normal-weight (20≦BMI<25)
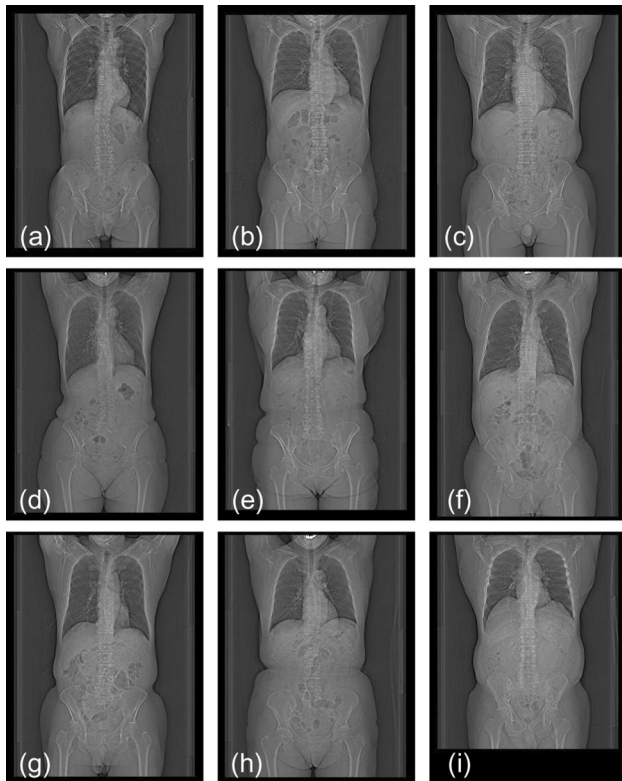c. Overweight (25≦BMI)
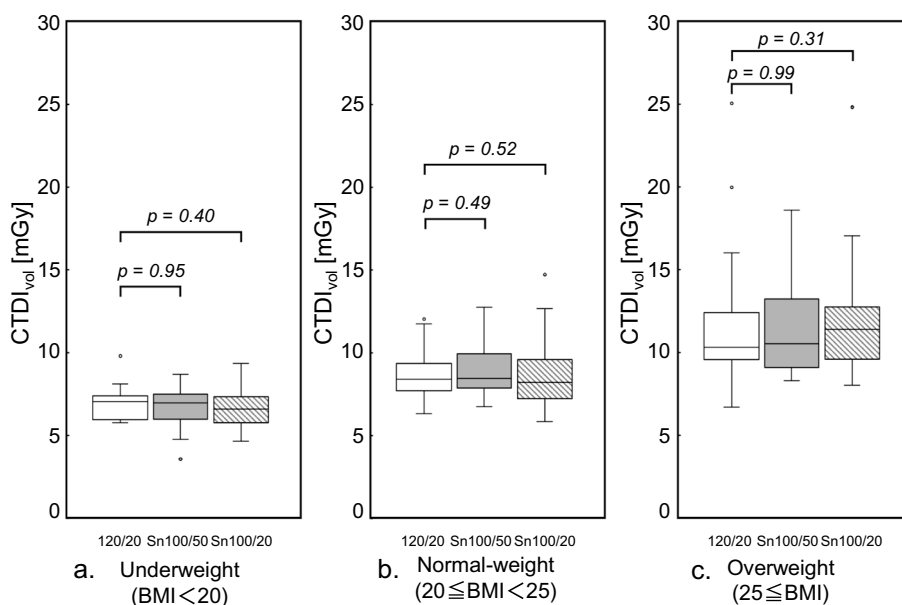
Fig. 3 LRs during chest–pelvis CT with **a** 120/20 protocol in underweight, **b** 120/20 protocol in normal-weight, **c** 120/20 protocol in overweight, **d** Sn100/50 protocol in underweight, **e** Sn100/50 protocol in normal-weight, **f** Sn100/50 protocol in overweight, **g** Sn100/20 protocol in underweight, **h** Sn100/20 protocol in normal-weight, and **i** Sn100/20 in overweight

the upper thoracic vertebrae was unclear in the LRs when the Sn100/50 protocol was applied in the normal-weight and overweight BMI groups, although the structures under other conditions were clearly observed.

Figure 6 shows the results of the head CT of the 120/20 and Sn100/50 protocols; the $CTDI_{vol}$s in the underweight

and overweight groups did not show significant differences (underweight: $p = 0.95$; overweight: $p = 0.36$). Meanwhile, for the normal-weight group, the $CTDI_{vol}$s of the Sn100/50 protocol were statistically lower than those of the 120/20 protocol (55.12 ± 2.81 mGy vs. 56.55 ± 3.31 mGy, $p = 0.02$). Typical images are shown in Fig. 7, in which the structure of the skull bone can be observed under all the conditions.

4 Discussion

In the present study, we found that tin filter technology can reduce ESD when acquiring LRs using an anthropomorphic phantom. We also investigated the effect of the scan conditions of the LRs on the performance of the ATCM using clinical datasets.

The LRs using the lowest radiation dose protocol (Sn100 kVp/20 mA) reduced the radiation dose by more than 90% compared to the dose in the conventional protocol without affecting the ATCM performance in all BMI groups performed chest–pelvis CT examinations. Furthermore, LRs acquired in the posteroanterior direction in clinical studies were assumed to reduce the radiation dose compared to that acquired in the anteroposterior direction in the phantom study because the radiation beam strikes the table first and the lowest energy X-rays are absorbed [6]. Moreover, the sensitive organs are located at the front of the body; therefore, the effective dose of LRs in the posteroanterior direction is expected to be lower than that in the anteroposterior direction [17]. Saltybaeva et al. showed that low-dose settings (Sn100 kVp/20 mA) affect ATCM performance in patients who are large due to the underestimation of attenuation [12]. This difference in the effect on the ATCM performance is believed to be due to the use of a phantom larger than the patient group of our facility in Japan. Therefore, we suggest using the lowest radiation dose protocol (Sn100

Fig. 4 Results of the clinical study during spine CT examinations. **a**, **b**, and **c** The box and whisker plots of $CTDI_{vol}$s for patients who were underweight, normal-weight, and overweight, respectively, in each protocol. There were statistical differences between the 120/20 and Sn100/50 protocols in the normal-weight and overweight groups **b**, **c**
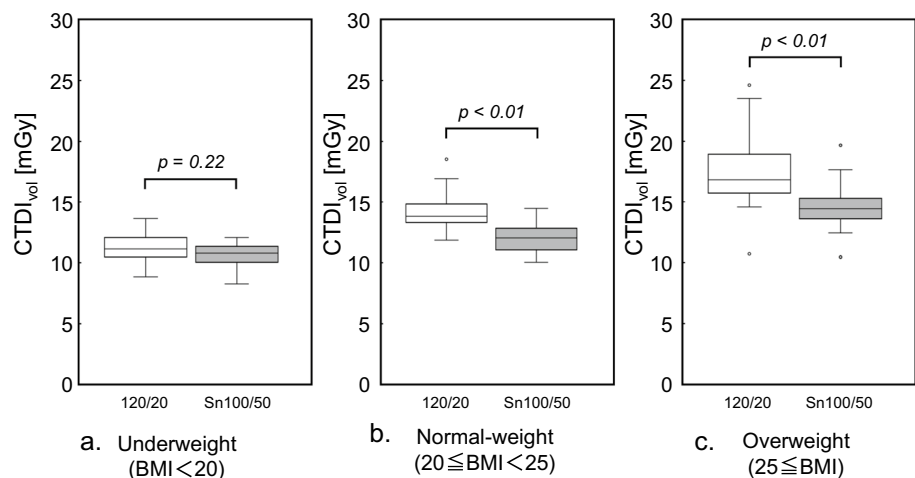
Fig. 5 LRs during spine CT with **a** 120/20 protocol in underweight, **b** 120/20 protocol in normal-weight, **c** 120/20 protocol in overweight, **d** Sn100/50 protocol in underweight, **e** Sn100/50 protocol in normal-weight, and **f** Sn100/50 protocol in overweight. The upper thoracic vertebrae were not visible with the Sn100/50 protocol in the normal-weight and overweight BMI groups (black arrow)
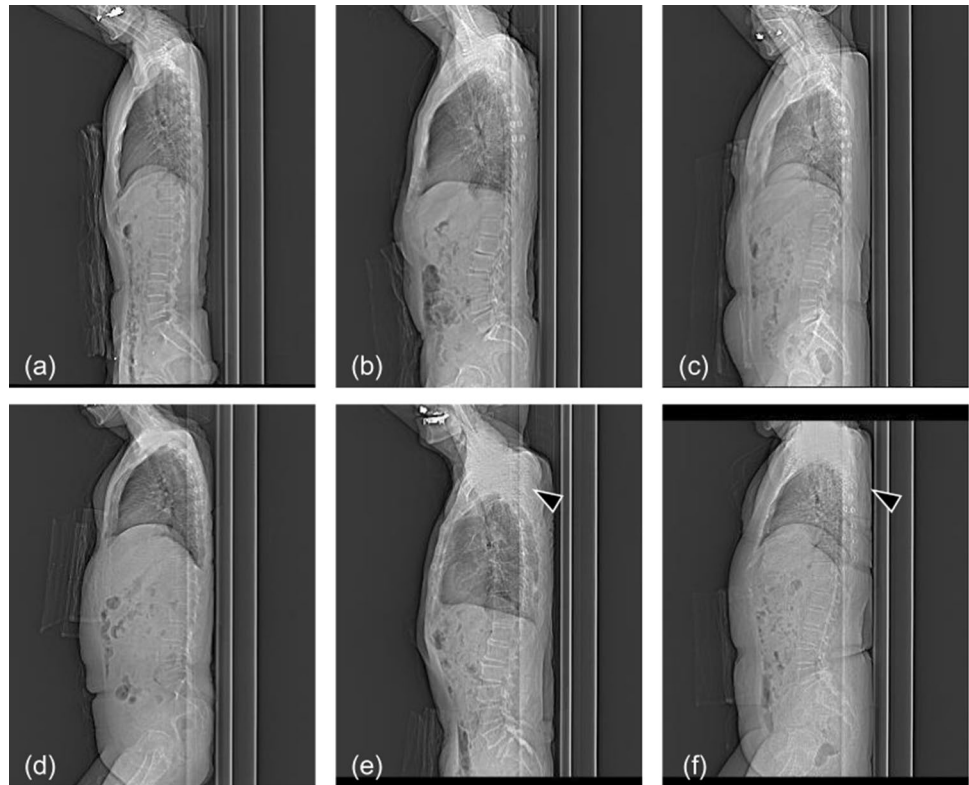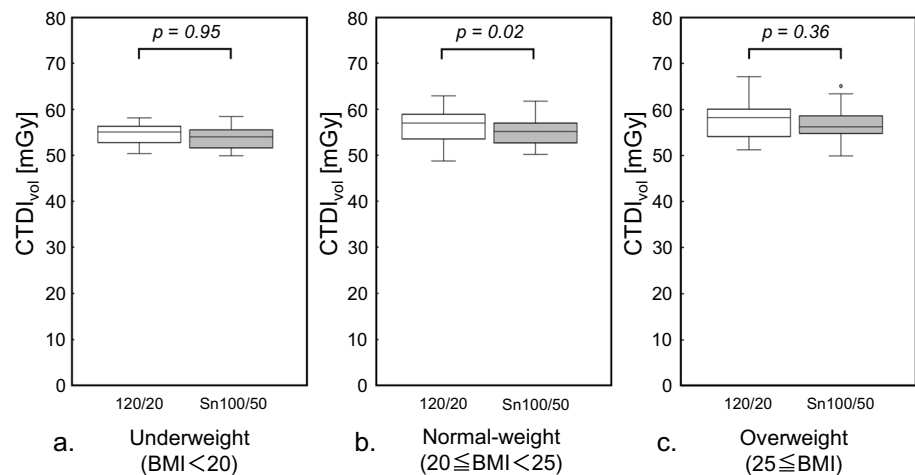

Fig. 6 Results of the clinical study during head CT examinations. **a**, **b**, and **c** The box and whisker plots of CTDI$_{vol}$s for patients who were underweight, normal-weight, and overweight, respectively, in each protocol. There was a statistical difference between the 120/20 and Sn100/50 protocols in the normal-weight group (**b**)


kVp/20 mA) when acquiring LRs in the posteroanterior direction in the Japanese population.

The results of spine CT examinations showed that LRs with a tin filter (Sn100 kVp/50 mA) affected ATCM performance in the normal-weight and overweight BMI groups. This was because the attenuation increased owing to the LRs performed in the lateral direction. We believed that the disappearance of anatomical landmarks meant a lack of signal (Fig. 5) and may suggest that tube current modulation in the region of the upper thoracic vertebrae was not performed properly in the groups with a BMI > 20. This is consistent

with the results reported by Bohrer et al. [11]. They reported that the lowest setting of the lateral LR (80 kVp/20 mA) leads to an effect on tube current modulation and that the lateral LR of the chest phantom required a higher tube voltage and tube current (100 kVp/20 mA) due to the high attenuation in the shoulder region. Furthermore, Saltybaeva et al. assumed that a suboptimal setting for the LRs in a large phantom led to a significant loss of the signal at the detector, resulting in incorrect implementation of the tube current modulation [12]. Therefore, the optimal acquisition setting for the lateral LR of spine CT examination needs to

Fig. 7 LRs during head CT with **a** 120/20 protocol in underweight, **b** 120/20 protocol in normal-weight, **c** 120/20 protocol in overweight, **d** Sn100/50 protocol in underweight, **e** Sn100/50 protocol in normal-weight, and **f** Sn100/50 protocol in overweight
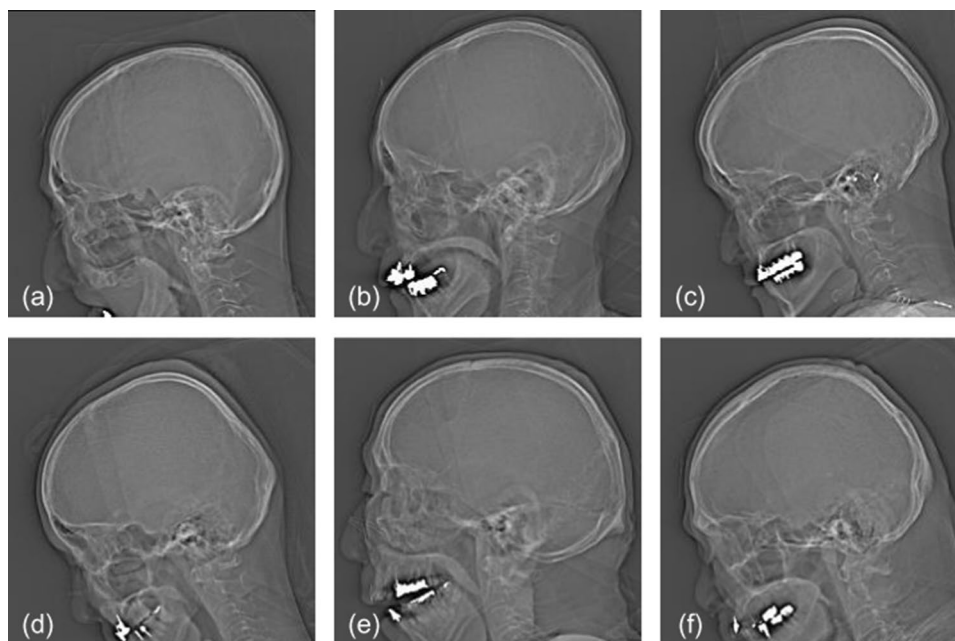
be determined with strategies such as increasing the tube voltage (Sn150 kVp) or tube currents or altering the ATCM setting to increase the exposure dose when using lateral LRs. Frank et al. reported that patient attenuation can be estimated more accurately by acquiring two orthogonal radiographs [18]. Radiation doses are sufficiently low even if two LRs are acquired in the orthogonal direction; therefore, we believe that adding the LR in the posteroanterior direction optimizes ATCM performance in spine CT examinations.

We found a statistical difference in $CTDI_{vol}$ between LRs with and without the tin filter on head CT examination for the normal-weight group ($20 \leq BMI < 25$). Brisse et al. reported that tube current modulation using the ATCM technique differed according to the tube potential of the LR [19]. We assumed that the signal values of the LRs changed because the tin filter technology alters the tube voltage and changes the X-ray spectrum. This was evident in regions with higher attenuation, such as the skull bones. However, the differences in the average values of the $CTDI_{vol}$s with and without the tin filter protocol were 1.43 mGy. This difference can be considered negligible in clinical situations.

Our study had several limitations. We investigated LRs using an additional filter made of tin for only one CT scanner from one vendor. We did not test our method using other machines or different filter materials. Therefore, our results may not be generalizable to other situations. Second, the patient population in our study was small, and consisted only of patients who were Japanese. Consequently, many patients in our study were lightweight, and we did not find an adequate scan setting for patients with a high BMI. Third, we did not evaluate the depth of dose absorbed by each patient's body. We only measured ESDs; therefore, a more comprehensive evaluation of the radiation dose from LRs is needed. Finally, we showed the feasibility of LR with a tin filter from the point of view of radiation dose and did not evaluate image quality in detail. Further investigation of image quality under clinical conditions is needed, taking into consideration the effects on ATCM performance.

5 Conclusion

Our study indicated that the ESD of LRs can be reduced to a maximum of 0.02 mGy when a tin filter is used. Furthermore, LRs with tin filter technology can reduce patient dosage for any region of CT examinations. However, we should optimize the scan setting for LRs or the ATCM setting for subsequent CT scans to avoid an effect on the performance of ATCM when patients have a BMI of ≥ 20 kg/m^2.

Declarations

Conflict of interest All the authors declare that they have no conflict of interest.

Ethical approval All the procedures performed in this study involving human participants were in accordance with the ethical standards of Institutional Review Board and with the 1964 Helsinki Declaration and its later amendments or comparable ethical standards. For this type of study, formal consent was not required at our institution.

References

1. Meinel FG, Canstein C, Schoepf UJ, et al. Image quality and radiation dose of low tube voltage 3rd generation dual-source coronary CT angiography in obese patients: a phantom study. Eur Radiol. 2014;24:1643–50.
2. Wuest W, May M, Saake M, et al. Low-dose CT of the paranasal sinuses: minimizing x-ray exposure with spectral shaping. Eur Radiol. 2016;26:4155–61.
3. Gordic S, Morsbach F, Schmidt B, et al. Ultralow-dose chest computed tomography for pulmonary nodule detection. Invest Radiol. 2014;49:465–73.
4. Haubenreisser H, Meyer M, Sudarski S, et al. Unenhanced third-generation dual-source chest CT using a tin filter for spectral shaping at 100 kVp. Eur J Radiol. 2015;84(8):1608–13.
5. Schmidt BT, Hupfer M, Saltybaeva N, et al. Dose optimization for computed tomography localizer radiographs for low-dose lung computed tomography examinations. Invest Radiol. 2017;52:81–6.
6. Daniel JC, Stevens DM, Cody DD. Reducing radiation exposure from survey CT scans. Am J Radiol. 2005;185:509–15.
7. Sato T, Kikuchi Y, Nakamura M, et al. Radiation exposure in computed tomography localizer radiograph. Jpn J Radiol Technol. 2019;75(12):1403–10.
8. Nowik P, Poludniowski G, Svensson A, et al. The synthetic localizer radiograph – a new CT scan planning method. Phys Med. 2019;61:58–63.
9. Perisinakis K, Damilakis J, Voloudaki A, et al. Patient dose reduction in CT examinations by optimising scanogram acquisition. Radiat Prot Dosim. 2001;93:173–8.
10. Nauer CB, Kellner-Weldon F, Von Allmen G, et al. Effective doses from scan projection radiographs of the head: impact of different scanning practices and comparison with conventional radiography. Am J Neuroradiol. 2009;30:155–9.
11. Boher E, Schafer S, Mader U, et al. Optimizing radiation exposure for CT localizer radiographs. Z Med Phys. 2017;27:145–58.
12. Saltybaeva N, Krauss A, Alkadhi H. Technical note: radiation dose reduction from computed tomography localizer radiographs using a tin spectral shaping filter. Med Phys. 2019;46(2):544–9.
13. Allmendinger T, Hamann A. Calcium scoring using tin filter spectral shaping a demonstration of Agatston equivalence. Siemens Healthcare GmbH. 2017. https://marketing.webassets.siemens-healthineers.com/1800000006813010/4de284a59358/siemens-healthineers-ct-somatom-drive-cascoring-tinfilter-white-paper_1800000006813010.pdf. Accessed 19 Dec 2022.
14. Woods M, Brehm M. Shaping the beam: Versatile filtration for unique diagnostic potential within Siemens Healthineers CT. Siemens Healthcare GmbH. 2019. https://cdn0.scrvt.com/39b415fb07de4d9656c7b516d8e2d907/1800000006857523/27030c03dfe2/siemens-healthineers-ct-technologies-and-innovations-tin-filter-whitepaper_v2_1800000006857523.pdf. Accessed 19 Dec 2022.
15. Takegami K, Hayashi H, Yamada K, et al. Entrance surface dose measurements using a small OSL dosimeter with a computed tomography scanner having 320 rows of detectors. Radiol Phys Technol. 2017;10:49–59.
16. Takegami K, Hayashi H, Asahara T, et al. Dose calibration factor of an OSL dosimeter during CT examination to measure expose dose of patients taking into consideration proper X-ray quality. Eur Congress Radiol. 2020;11:01393.
17. Schmidt B, Saltybaeva N, Kolditz D, et al. Assessment of patient dose from CT localizer radiographs. Med Phys. 2013;40(8):084301.
18. Frank C, Bacher K. Influence of localizer and scan direction on the dose-reducing effect of automatic tube current modulation in computed tomography. Radiat Prot Dosim. 2016;169:136–42.
19. Brisse HJ, Ma Dec L, Gaboriaud G, et al. Automatic exposure control in multichannel CT with tube current modulation to achieve a constant level of image noise: experimental assessment on pediatric phantoms. Med Phys. 2007;34(7):3018–33.